Flavonoid-Capped Gold Nanoparticles from *Boesenbergia rotunda*: Enhanced Antioxidant Activity and Cyclin-Dependent Kinase 2 (CDK2) Inhibition via Molecular Docking

Dini Nur Fauzia[1,2], Afaf Baktir[2], Titik Taufikurohmah[3], Intan Permata Sari[4], Dzikra Nasyaya Mahfudhah[4], and Mochamad Zakki Fahmi[2*]

[1]*Doctoral Program of Mathematics and Natural Sciences, Faculty of Science and Technology, Universitas Airlangga, Jl. Dr. Ir. H. Soekarno, Mulyorejo, Surabaya 60115, Indonesia*

[2]*Department of Chemistry, Faculty of Science and Technology, Universitas Airlangga, Jl. Dr. Ir. H. Soekarno, Mulyorejo, Surabaya 60115, Indonesia*

[3]*Department of Chemistry, Faculty of Mathematics and Natural Sciences, Universitas Negeri Surabaya, Jl. Ketintang, Surabaya 60231, Indonesia*

[4]*Master's Program in Chemistry, Faculty of Science and Technology, Universitas Airlangga, Jl. Dr. Ir. H. Soekarno, Mulyorejo, Surabaya 60115, Indonesia*

* ***Corresponding author:***

tel: +62-83832901697
email: m.zakki.fahmi@fst.unair.ac.id

Received: January 26, 2026
Accepted: April 23, 2026

DOI: 10.22146/ijc.116010

Abstract: *The green synthesis of gold nanoparticles (Br-AuNPs) using ethanolic extracts of* Boesenbergia rotunda *offers an eco-friendly approach to producing bioactive nanomaterials. This study aimed to synthesize Br-AuNPs and evaluate their antioxidant activity alongside* in silico *analysis of flavonoid interactions with the CDK2/cyclin A complex. The formation of Br-AuNPs was confirmed by a visible color change and a distinct SPR peak at 538–542 nm. TEM analysis revealed spherical nanoparticles with an average diameter of 14.35 ± 3.16 nm, stable for up to four months. Antioxidant activity assessed via the ABTS assay showed that Br-AuNPs exhibited significantly higher radical scavenging activity (69.01% at 120 μg/mL) compared to the crude extract (56.0%; $p < 0.05$). This enhancement is attributed to synergistic interactions between phytochemicals and nanoparticles, which improve surface reactivity. Furthermore, molecular docking studies were conducted to evaluate the interaction of major flavonoids from* B. rotunda *with the CDK2/cyclin A complex, where 6,8-di-(3,3-dimethylallyl)chrysin showed the most favorable binding affinity (−63.30 kcal/mol). These findings highlight the potential of Br-AuNPs as green-synthesized nanomaterials with enhanced antioxidant performance and provide a scientific basis for future investigations toward their development in anticancer-related applications.*

Keywords: Boesenbergia rotunda*; gold nanoparticles; flavonoids; molecular docking; anticancer activity*

■ INTRODUCTION

The rapid advancement of nanotechnology has created new possibilities for the development of functional nanomaterials in biomedicine, particularly in cancer therapy [1-3]. In the field of nanomaterials, AuNPs have received widespread attention in recent times, resulting from their distinctive physicochemical properties and broad applications in medicine, diagnostics, and biotechnology [1,4-5]. AuNP-based colorimetric systems have also been reported as simple, rapid approaches for selective analyte detection via nanoparticle aggregation-induced color changes [6]. Owing to their tunable optical properties, large surface area, and biocompatibility, AuNPs hold great potential in drug delivery, imaging, biosensing, and anticancer therapies [7-8]. In recent

years, green synthesis or biofabrication of AuNPs using plant-derived phytochemicals has gained significant interest as an eco-friendly, cost-effective, and sustainable approach compared to conventional physical and chemical methods [9-12]. The green synthesis of nanoparticles using plant extracts, known as phytofabrication, combines eco-friendly chemistry with biofunctionalization, where phytochemicals serve dual roles as reducers and stabilizers. This approach enables the fabrication of bioactive nanomaterials that retain the therapeutic potential of their botanical sources [12-14].

The flavonoid *Boesenbergia rotunda* (L.) Mansf. has traditionally been applied in Southeast Asian traditional medicine. It contains abundant bioactive phytochemicals, particularly flavonoids. Flavonoids, a class of polyphenolic compounds ubiquitously present in plants used in medicinal plants traditionally used in herbal medicine, have been recognized as effective reducing and capping agents in the green synthesis of AuNPs [13,15-16]. These flavonoids such as pinostrobin, panduratin A, and various prenylated chalcones and flavones, display diverse biological activities, including antioxidant and anti-inflammatory effects, antibacterial, and anticancer properties [17-19]. These secondary metabolites act as reducing and capping agents for the biosynthesis of metal nanoparticles, providing both stability and functional surface chemistry conducive to biological applications. Other flavonoids that exhibit promising anticancer potential through diverse biological mechanisms, including cell cycle inhibition and promoting apoptosis [20-22]. In particular, pinostrobin has been reported to show antiproliferative activity and induce apoptosis in cancer cells through ROS-dependent mechanisms and cell-cycle regulation pathways [23-25].

Natural products and phytochemicals are increasingly explored as pharmaceutical candidates owing to their superior biocompatibility and reduced toxicity relative to chemically synthesized counterparts. This approach is favored due to its minimal adverse effects and lower toxicity compared to conventional chemotherapeutics, although its clinical application remains constrained by poor solubility and limited bioavailability [26-27]. AuNPs represent an emerging nanocarrier platform that improves the solubility and bioavailability of natural bioactive substances, positioning them as effective candidates for drug delivery systems [5,13,28]. Flavonoid or phenolic-based nanomedicines offer a potential approach for advancing novel anticancer, antioxidant, and antibiofilm agents that may complement conventional therapies [29-30]. Recent advances have shown that flavonoid-functionalized AuNPs can serve dual roles: as carriers and as active agents with intrinsic anticancer properties [26-27]. In this context, *B. rotunda* represents a valuable, promising agent for the synthesis of multifunctional AuNPs because of its rich repertoire of bioactive secondary metabolites. However, the mechanistic understanding of how these flavonoids interact with cancer-related molecular targets remains limited. Flavonoids have been widely reported to modulate key molecular pathways in cancer, including cell cycle regulation, oxidative stress, angiogenesis, and metastasis, thereby contributing to cancer prevention [18,31-32]. Epidemiological studies associate flavonoid-rich diets with a reduced risk of breast, skin, gastrointestinal, hematological, and prostatic carcinoma [33-34].

In cancer treatment, cyclin-dependent kinase 2 (CDK2) plays a key role in controlling cell cycle progression, especially the G1 to S phase transition. Overexpression or dysregulation of CDK2/cyclin A complex has been associated with various human malignancies, making it a critical target for anticancer drug development [35-36]. Cyclin-dependent kinase 2 (CDK2), particularly in complex with cyclin A, is a pivotal regulator of cell cycle progression through the G1/S and S phases. Its aberrant activity and overexpression have been strongly correlated with tumor proliferation in various human cancers, making the CDK2/cyclin A complex an attractive therapeutic target [35-38]. Molecular docking is a widely used *in silico* approach to estimate the binding strength and molecular interactions of small molecules with biological targets, providing valuable insights into their potential mechanism of action and guiding rational drug design [35,39]. The CDK2/cyclin A complex plays a pivotal role in controlling cell cycle progression, especially the G1 to S phase transition, and has attracted

considerable attention as a candidate for therapeutic intervention in anticancer drug discovery. Several previous *in silico* studies have demonstrated that both natural and synthetic compounds can inhibit CDK2 activity by binding to its ATP-binding site, thereby disrupting kinase function [36-37,40]. Flavonoids such as kaempferol, quercetin and apigenin have also exhibited favorable docking scores and stable interactions with key active site residues of CDK2, suggesting their potential as selective inhibitors [40-43]. However, studies focusing on flavonoids from *B. rotunda* as inhibitors of the CDK2/cyclin A complex remain very limited. Despite its pharmacological potential, no studies to date have reported the conjugation of *B. rotunda* flavonoids with AuNPs, leaving a notable gap in the integration of its phytochemicals with nanotechnology-based delivery systems. Additionally, the molecular interaction of these flavonoids with key regulatory proteins such as CDK2 remains largely unexplored. Given the increasing interest in natural compounds as potential CDK2 inhibitors, the present study is directed toward exploring the binding affinity and interaction profiles of major *B. rotunda* flavonoids through molecular docking analysis. The findings are expected to provide preliminary insight into their suitability as molecular scaffolds for the future development of flavonoid-capped AuNPs targeting CDK2.

Here, we reveal for the first time the plant-mediated biosynthesis of gold nanoparticles through ethanolic extract of *B. rotunda* (Br-AuNPs), assess their physicochemical traits and evaluate the antioxidant and anticancer activity of flavonoids via molecular docking against the CDK2/cyclin A complex (PDB ID: 6GUB), highlighting their promise as kinase inhibitors. The synthesized Br-AuNPs were evaluated using UV-vis, FTIR, DLS, and TEM, revealing stable spherical AuNPs with a distinct surface plasmon resonance and nanometric size. A panel of major *B. rotunda* flavonoids was docked into the CDK2/cyclin A active site to assess their binding affinities, interaction modes, and comparative potential against a known inhibitor, flavopiridol. This study adopts an integrative approach combining green synthesis of flavonoid-mediated AuNPs, antioxidant evaluation, and *in silico* molecular docking analysis targeting the CDK2/Cyclin A complex, providing preliminary insights into their multifunctional potential in nanomedicine applications.

■ EXPERIMENTAL SECTION

Materials

B. rotunda rhizomes were collected from a local herbal market in East Java, Indonesia. Chloroauric acid ($HAuCl_4$), 2,2′-azino-bis(3-ethylbenzothiazoline-6-sulfonic acid (ABTS), potassium persulfate ($K_2S_2O_8$) and potassium bromide (KBr) were obtained from Sigma-Aldrich (USA), while absolute ethanol and methanol were obtained from Merck (Germany). All reagents employed in this study were of analytical grade.

Instrumentation

The optical characteristics of the synthesized Br-AuNPs were examined through UV–vis spectroscopy using a GENEYSYS 150 spectrophotometer (Thermo Scientific, USA). FTIR spectra were determined with a Perkin Elmer Spectrum One system (Perkin Elmer, USA) to identify functional groups associated with the nanoparticle surfaces. Morphological features were visualized by TEM employing a Jeol JEM-1400 microscope operated at 120 kV (Jeol, Japan) for high-resolution imaging. The hydrodynamic diameter distribution was assessed via dynamic light scattering (DLS) using a BIOBASE Nano Particle Size Analyzer (Biobase Biodustry, China), providing reliable information on the colloidal characteristics.

Procedure

Preparation of B. rotunda *extract*

The fresh rhizomes of *B. rotunda* were carefully cleaned, air-dried, and pulverized into a fine powder. A total of 200 g of the powdered sample was extracted with 500 mL of ethanol by maceration for 24 h. The filtrate was subsequently concentrated using a rotary vacuum evaporator maintained at 70 °C for 1 h and then stored at 4 °C for future use [44-45].

Bio-fabrication of AuNPs using B. rotunda *extract*

The biosynthesis of Br-AuNPs was carried out by adding 1 mL of *B. rotunda* extract to 90 mL of 1 mM aqueous $HAuCl_4$ solution, followed by continuous

stirring at room temperature. The obtained reaction system was observed for a chromatic transition from pale yellow to red-purple, subsequent to a duration of 15 min, signifying the synthesis of AuNPs [1-2,12,46]. The obtained nanoparticles were separated by centrifugation at 12,000 rpm for 15 min, rinsed with deionized water, and subsequently dried in a vacuum desiccator [3].

Molecular docking analysis

Major flavonoids reported from *B. rotunda*, particularly from its ethanolic extracts, were selected as ligands for docking simulation. Molecular docking was performed using Dock 6.8 software. Protein molecules were prepared and their surfaces generated in Chimera 1.16, utilizing the Dock Prep and Write DMS modules. Spherical models were constructed using SPHGEN, and the active site was an 8.0 Å radius from the native ligand using SPHERE_SELECTOR. The docking box was created using SHOWBOX with an additional 8.0 Å margin, and a grid with 0.25 Å resolution was generated using the GRID module [47-49].

ABTS radical scavenging assay

The antioxidant activity of Br-AuNPs and *B. rotunda* extract was evaluated using the ABTS assay following a previously reported method [50] with slight modifications. The ABTS radical cation ($ABTS^{\bullet+}$) was prepared by reacting 7 mM ABTS with 140 mM $K_2S_2O_8$ and incubated in the dark at room temperature for 12–16 h. The solution was diluted with ethanol to an absorbance of 0.70 ± 0.02 at 734 nm. The reaction mixture consisted of 1 mL $ABTS^{\bullet+}$ solution and 10 µL of the sample. After incubation at 30 °C for 4 min, absorbance was measured at 734 nm using a UV-vis spectrophotometer. Antioxidant activity was expressed as the decrease in $ABTS^{\bullet+}$ absorbance, where a greater reduction indicates higher radical scavenging activity. All measurements were performed in triplicate.

■ RESULTS AND DISCUSSION

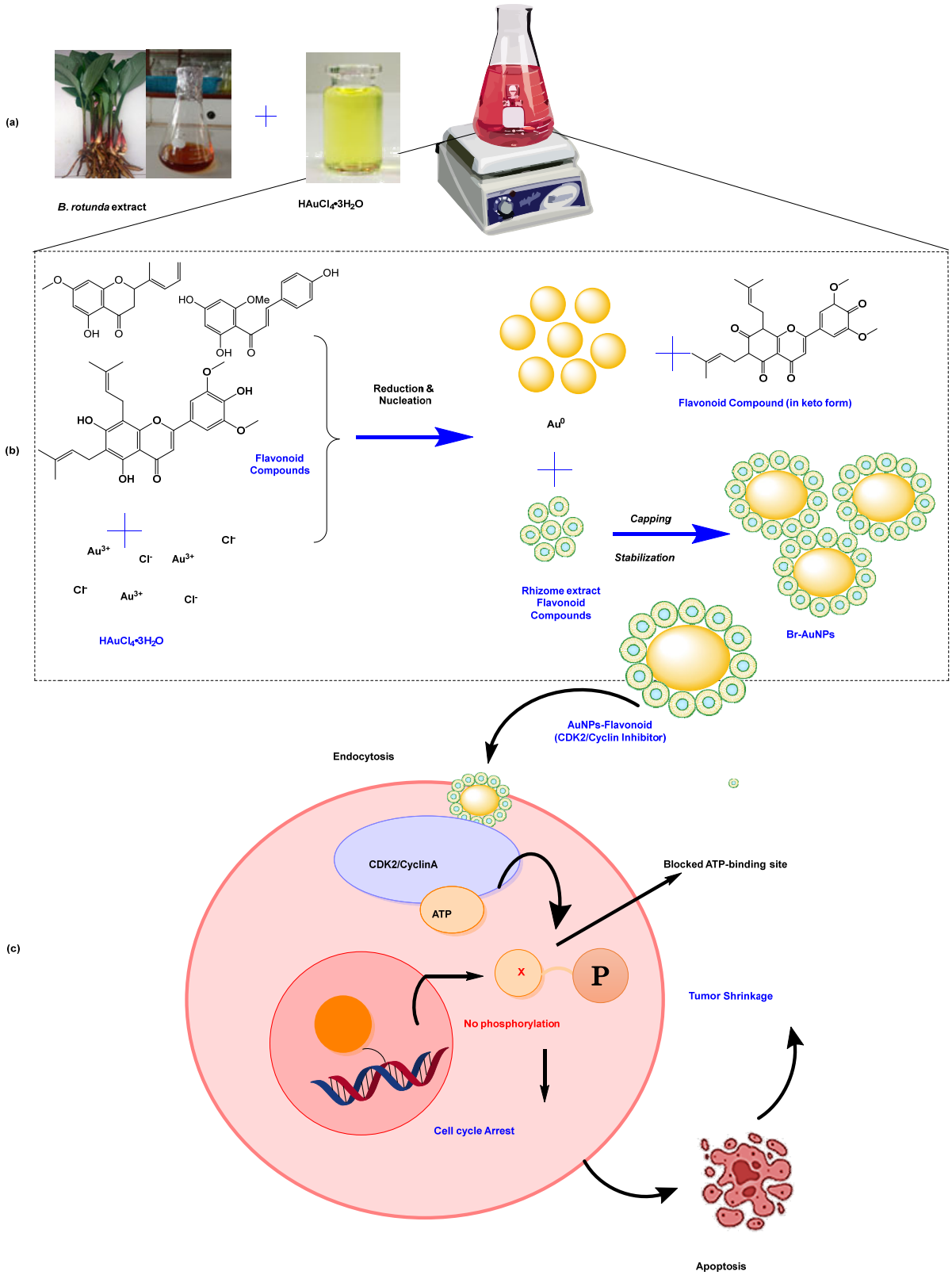
Green Synthesis of AuNPs Mediated by *B. rotunda* Extract

AuNPs were successfully biosynthesized using *B. rotunda* rhizome extract, which was achieved through the conversion of Au^{3+} ions by phytochemicals contained in the extract, particularly flavonoids, causing the production of Br-AuNPs. When the extract was added to an aqueous $HAuCl_4$ solution, the color instantly changed from yellow to pale pink and progressively developed into red-purple, indicating the nucleation and growth of AuNPs [6,50]. The development of a red-purple coloration is characteristic of the surface plasmon resonance (SPR) associated with AuNPs formation, suggesting the successful reduction and stabilization of Au^{3+} ions by bioactive constituents [51-52]. The freeze-dried product obtained from 90 mL of colloidal solution yielded approximately 3 mg of dried Br-AuNPs, corresponding to an estimated concentration of 0.033 mg/mL. This value should be considered semi-quantitative, as it may be influenced by material loss during purification and the presence of phytochemical capping layers on the nanoparticle surface.

The biosynthesis process was initially monitored through visual observation, and a schematic representation of the green synthesis mechanism is presented in Scheme 1. Moreover, Scheme 1 presents the suggested mechanism for the biosynthesis of Br-AuNPs mediated by phytochemicals present in *B. rotunda* rhizome extract. The major constituents, particularly flavonoids (e.g., pinostrobin, pinocembrin, alpinetin, and chrysin) are considered key contributors to nanoparticle formation [13]. These polyphenols not only act as reducing agents by converting Au^{3+} ions into metallic Au^0 but also function as stabilizers, forming a protective layer on the nanoparticle surface to prevent agglomeration [53].

Characterization of Synthesis AuNPs

The synthesized AuNPs were analyzed using a range of spectroscopic and microscopic techniques to confirm their successful formation, evaluate their stability, and determine their structural and functional characteristics. It was monitored by UV-vis spectroscopy to confirm the formation. After adding rhizome extracts with $HAuCl_4$ solution, the color change observed was the



Scheme 1. (a) Illustration of AuNPs biosynthesis mediated by *B. rotunda* rhizome extract. (b) Proposed mechanism of Br-AuNPs formation, depicting the reduction and stabilization roles of phytochemicals in the extract. (c) Graphical representation of Br-AuNPs CDK2 inhibition thereby inducing cell cycle arrest and apoptosis in cancer cells

biotransformation of Au^{3+} ions into atomic clusters (AuNPs). The red-purple color appears (Fig. 1(a)) due to the SPR phenomenon. UV-vis spectra of the AuNPs displayed a distinct SPR peak at around 538–542 nm (Fig. 1(b)), which is particularly recognized for AuNPs. We observe that this peak corresponds to SPR, which represents a unique characteristic property exclusive to metallic nanoparticles like gold [54]. The findings align with earlier studies, which reported that AuNPs synthesized employing *Ziziphus spina-christi* leaf extract and dried fruit extract of *Capsicum annuum* both exhibited an absorption peak at 540 nm and remained stable for up to 3 months [9]. The distinct SPR peak indicates uniform, reproducible AuNPs with good dispersion, while also confirming the phytochemical-mediated formation of metallic Au^0 from Au^{3+} ions by *B. rotunda* rhizome extract [12].

FTIR analysis was conducted to identify functional moieties contributing to the biosynthesis and stabilization of Br-AuNPs derived from *B. rotunda* rhizome extract. The spectra exhibited distinct peaks corresponding to hydroxyl (3471 cm^{-1}) and carbonyl groups (1630 cm^{-1}), confirming the role of these phytochemicals in nanoparticle formation. (Fig. 2(a–b)). These functional groups, typical of flavonoids and related phytochemicals, indicate that *B. rotunda* extract compounds participate in nanoparticle formation, where O–H groups function as reducing agents and C=O groups as stabilizing ligands, appear to serve dual roles as reductants and stabilizers in AuNP formation [13].

After the formation of AuNPs, slight shifts and reductions in the intensity of these bands were observed,

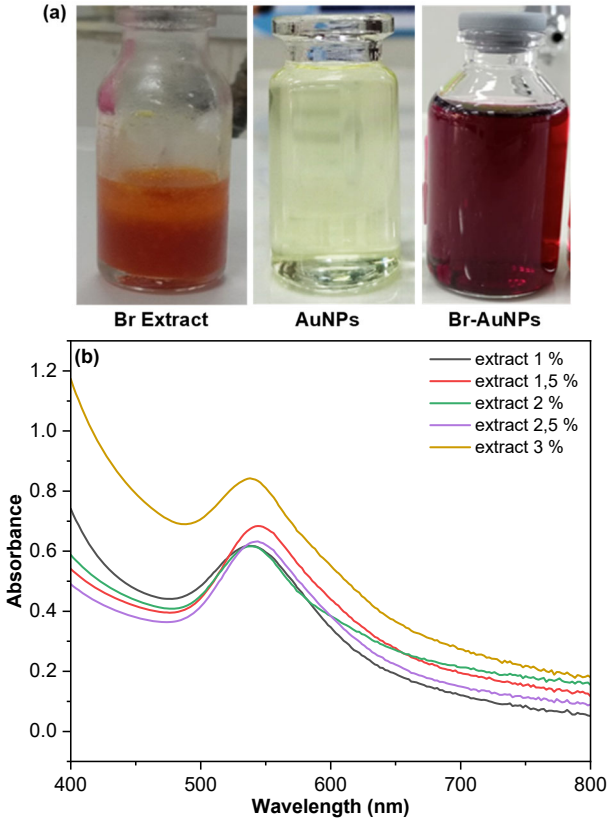


Fig 1. (a) Bio-reduction of *B. rotunda* extract into AuNPs with $HAuCl_4$ and (b) UV-vis spectra of Br-AuNPs (SPR peak at 538–542 nm)

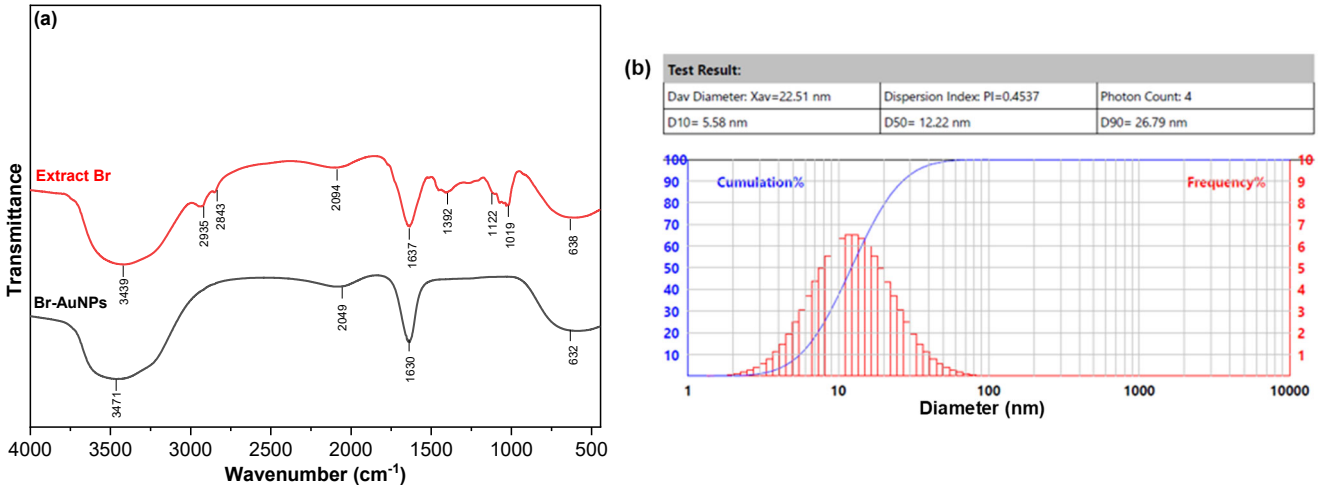


Fig 2. (a) FTIR spectra of Br-AuNPs and extract Br; and (b) dynamic light scattering (DLS) analysis of the Br-AuNPs

particularly in the O–H and C=O regions. These changes indicate the participation of hydroxyl and carbonyl groups in interactions with the nanoparticle surface, possibly through coordination interactions (Au–O) and hydrogen bonding. These functional groups are commonly associated with phenolic compounds, including flavonoids and related phytochemicals, which may contribute to both the reduction and stabilization processes during AuNP formation. The O–H groups are likely involved in electron donation during reduction, while C=O groups may assist in stabilizing the nanoparticle surface.

The presence of these functional groups on the nanoparticle surface confirms that phytochemicals from *B. rotunda* extract acted as effective capping agents, thereby preventing particle aggregation and improving colloidal stability [55]. The hydrodynamic diameter of phytochemically synthesized Br-AuNPs was evaluated using DLS, showing an average size of approximately 22.51 nm with a polydispersity index (PDI) of 0.45, indicating a moderately broad size distribution. The morphology and particle size were further examined using TEM [56,60]. As shown in Fig. 3(a–e), TEM analysis indicated that the synthesized AuNPs exhibited a predominantly spherical nanoparticles with an average diameter of 14.35 ± 3.16 nm. The larger size observed in DLS compared to TEM is attributed to the hydrodynamic diameter, which includes the nanoparticle core along with the surrounding solvation layer and phytochemical capping agents on the surface [12,17]. This difference is observed in phytochemically synthesized nanoparticles and reflects the presence of bioactive compounds stabilizing the system.

The colloidal stability of Br-AuNPs was inferred from their relatively uniform dispersion and the absence of visible aggregation over time. However, it should be noted that zeta potential measurements were not performed in this study, which represents a limitation in quantitatively assessing the colloidal stability of the nanoparticles.

Stability of Bio-Fabricated Br-AuNPs

The stability of Br-AuNPs was evaluated over a 4-month period under ambient storage conditions using UV-vis spectroscopy. The SPR peak remained within the range of 538–546 nm without significant shifts or peak

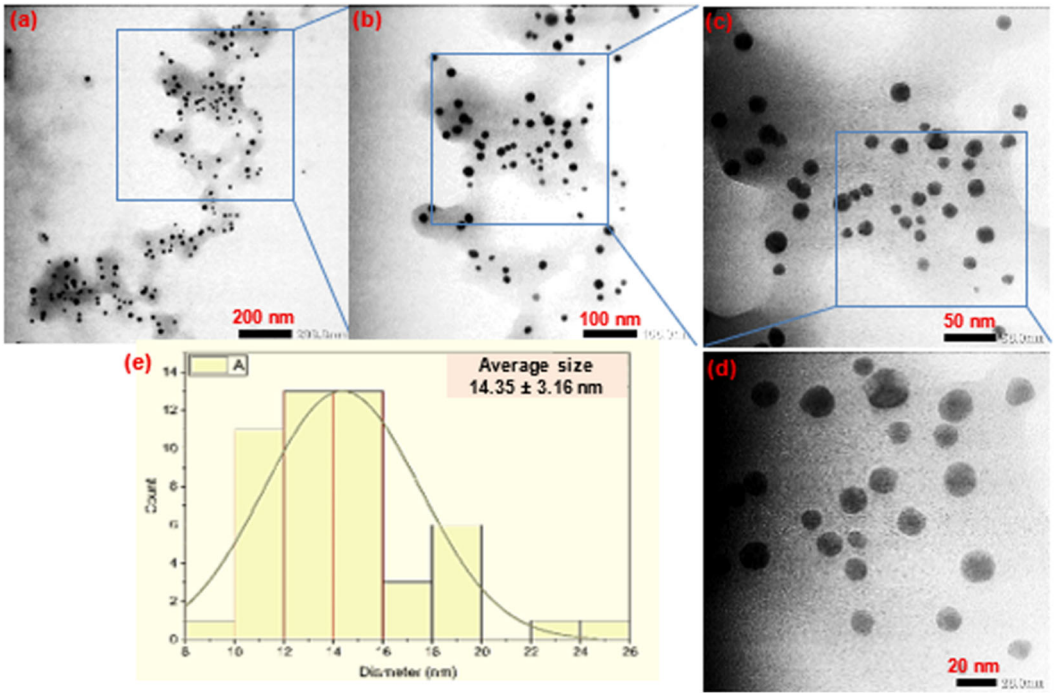


Fig 3. Representative TEM images of Br-AuNPs at scales of (a) 200, (b) 100, (c) 50, and (d) 20 nm, along with (e) a histogram the particle size distribution

broadening, indicating that the nanoparticles retained their structural integrity and did not undergo noticeable aggregation [55,58]. This stability is likely attributed to the capping effect of phytochemicals present in *B. rotunda* extract, particularly flavonoids containing hydroxyl and carbonyl groups, which can interact with the nanoparticle surface and provide steric stabilization [58-59]. DLS analysis showed that the hydrodynamic diameter remained relatively consistent over time, with a PDI of 0.45, indicating a moderately broad size distribution. These results suggest that the nanoparticles remained reasonably dispersed during storage [55,60]. However, it should be noted that zeta potential measurements were not performed in this study, which represents a limitation in quantitatively assessing the colloidal stability of the Br-AuNPs.

Molecular Docking and Binding Interaction with CDK2/Cyclin A

Validation of the docking protocol

The protocol was validated via native ligand redocking within the CDK2/cyclin A complex (PDB ID: 6GUB). The resulting pose was compared to the crystallographic conformation, and the root mean square deviation (HA_RMSDh) was calculated to be 0.409 Å, a Lennard-Jones potential score of 6–9, and a grid score of −75.07, indicating that the docking protocol is considered reliable. This RMSD value is well below the generally accepted threshold of 2.0 Å, indicating that the docking method can reliably reproduce the experimental binding mode [47-48]. Additionally, a grid score of −75.07 was obtained, supporting the predicted binding conformation. The structural alignment between the experimental (brown) and redocked (cyan) poses further supports the robustness of the docking setup, showing minimal deviation (Fig. 4). This validates the protocol for subsequent virtual screening and molecular docking simulations with candidate flavonoid ligands. Therefore, the docking protocol is considered valid and suitable for further virtual screening studies.

Molecular docking analysis

Earlier investigations have indicated that the ethanol extract of *B. rotunda* contains several flavonoids, including pinostrobin, alpinetin, chrysin, and pinocembrin [61]. These compounds were docked against the CDK2/cyclin A complex to evaluate their binding potential. The results showed that these flavonoids had potential interactions with ATP-binding pocket of CDK2. The integration of flavonoids with AuNPs in this study is proposed as a strategy to enhance their physicochemical properties; however, this aspect was not directly evaluated and requires further investigation.

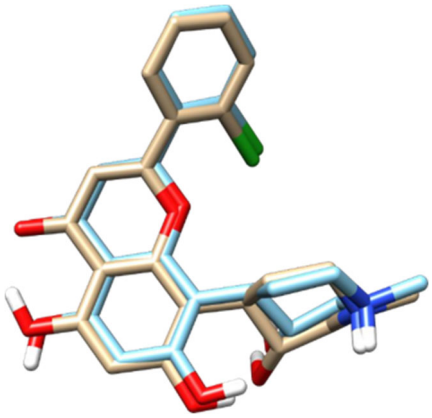


Fig 4. Superimposed binding poses of redocked flavopiridol (cyan) and crystallographic flavopiridol (brown) within the CDK2/cyclin A binding site, validating the docking protocol through close positional overlap

The assayed docking scores for each flavonoid compound interacting with the CDK2/cyclin A complex are summarized in Table 1 and visualized in Fig. 5 and 6. The docking scores (gridscore) obtained in this study ranged from −30.29 to −63.30, reflecting the relative binding potential of the tested flavonoids toward the CDK2/cyclin A complex, where more negative values indicate stronger predicted interactions. However, it should be noted that these values are derived from computational scoring functions and do not represent absolute binding free energies; therefore, they should be interpreted comparatively rather than quantitatively. Among the tested compounds, 6,8-di-(3,3-dimethylallyl) chrysin (compound 14) showed the lowest gridscore (−63.30), indicating the relatively strongest predicted interaction among the tested flavonoids within the ATP-binding pocket of CDK2. Nevertheless, its binding affinity remains lower than that of the reference ligand flavopiridol (−75.07), suggesting a moderate binding potential. The interaction involves

Table 1. Molecular docking analysis and amino acid interaction of *B. rotunda* flavonoids with CDK2/cyclin A

Ligand name	Grid score (kcal/mol)	Key H-bond residues	Hydrophobic interactions	π–π Stacking
R-Pinostrobin	−48.72	Glu82, Leu84	Ile11, Ala32, Phe81, Leu135	Phe81
S-Pinostrobin	−51.51	Lys34	Tyr16, Val19, Ala32, Leu135	–
R-Pinocembrin	−46.42	Glu82, Leu84	Ala32, Leu135	–
S-Pinocembrin	−49.56	Lys34	Val19, Ala32, Leu135	–
R-Alpinetin	−46.50	Glu82, Leu84	Ile11, Ala32, Leu135	–
S-Alpinetin	−46.61	Lys34	Tyr16, Val19, Ala32, Leu135	–
2',4'-dihydroxy-6-methoxychalcone	−49.29	Glu82, Leu84	Ala32, Leu135	Tyr16
(2*R*,7"*S*)-Pinocembrin derivative	−61.61	Lys34	Ile11, Tyr16, Val19, Ala31, Phe81, Leu135	Phe81
(2*R*)-Flavanone derivative	−43.71	Tyr16	–	–
S-Flavanone derivative	−46.00	Lys34	Tyr16, Val19, Ala32, Leu135	–
R-Flavanone derivative	−42.03	–	–	–
S-Dihydrofuranone	−30.92	Lys34	–	–
R-Dihydrofuranone	−30.29	Lys34	–	–
6,8-di-(3,3-dimethylallyl)chrysin	−63.30	Lys34	Ile11, Gly12, Leu135	–
R-Trihydroxy-prenylflavanone	−52.37	–	–	–
S-Trihydroxy-prenylflavanone	−59.12	Leu84, Gln132	Val65, Phe81, Leu135	–
2',6'-dihydroxy-4'-methoxydihydrochalcone	−51.23	Lys34	–	Phe81
Flavopiridol (native ligand)	−75.07	Lys34, Glu82, Leu84, Asp146	Ile11, Ala32, Leu135	Phe81

key residues such as Lys34, Ile11, Gly12, and Leu135, primarily via hydrogen bonding and hydrophobic interactions.

The interaction pattern of this compound shows similarity to that of flavopiridol, the reference ligand, particularly in forming hydrogen bonds and π–π interactions within the active site. However, it should be emphasized that these results represent preliminary *in silico* predictions and do not confirm actual inhibitory activity. Therefore, further experimental validation, including *in vitro* and *in vivo* studies, is required to confirm the biological relevance of these findings.

Other compounds, including *R*-pinostrobin (1), *S*-pinocembrin (4), *S*-alpinetin (6), 2',4'-dihydroxy-6-methoxychalcone (compound 8), and 2',6'-dihydroxy-4'-methoxydihydrochalcone, also demonstrated relevant interactions with the CDK2/cyclin A binding site. These interactions primarily involved hydrogen bonding and π–π stacking with key residues such as Glu82, Leu84, and Phe81. The presence of prenyl and hydroxyl groups in the flavonoid structures may contribute to these interactions by facilitating π–π stacking and hydrogen bonding. However, their interaction profiles were relatively weaker compared to that of flavopiridol, the reference ligand. These findings indicate that *B. rotunda* contains structurally diverse flavonoids with the potential to interact with the CDK2 active site. Nevertheless, it should be emphasized that these results are based on *in silico* predictions and do not confirm actual inhibitory activity. Further experimental validation is required to establish their relevance in anticancer applications.

In this study, molecular docking analysis was performed on free flavonoid compounds to evaluate their potential interaction with the CDK2 active site. The role of AuNPs is proposed as a delivery platform to improve

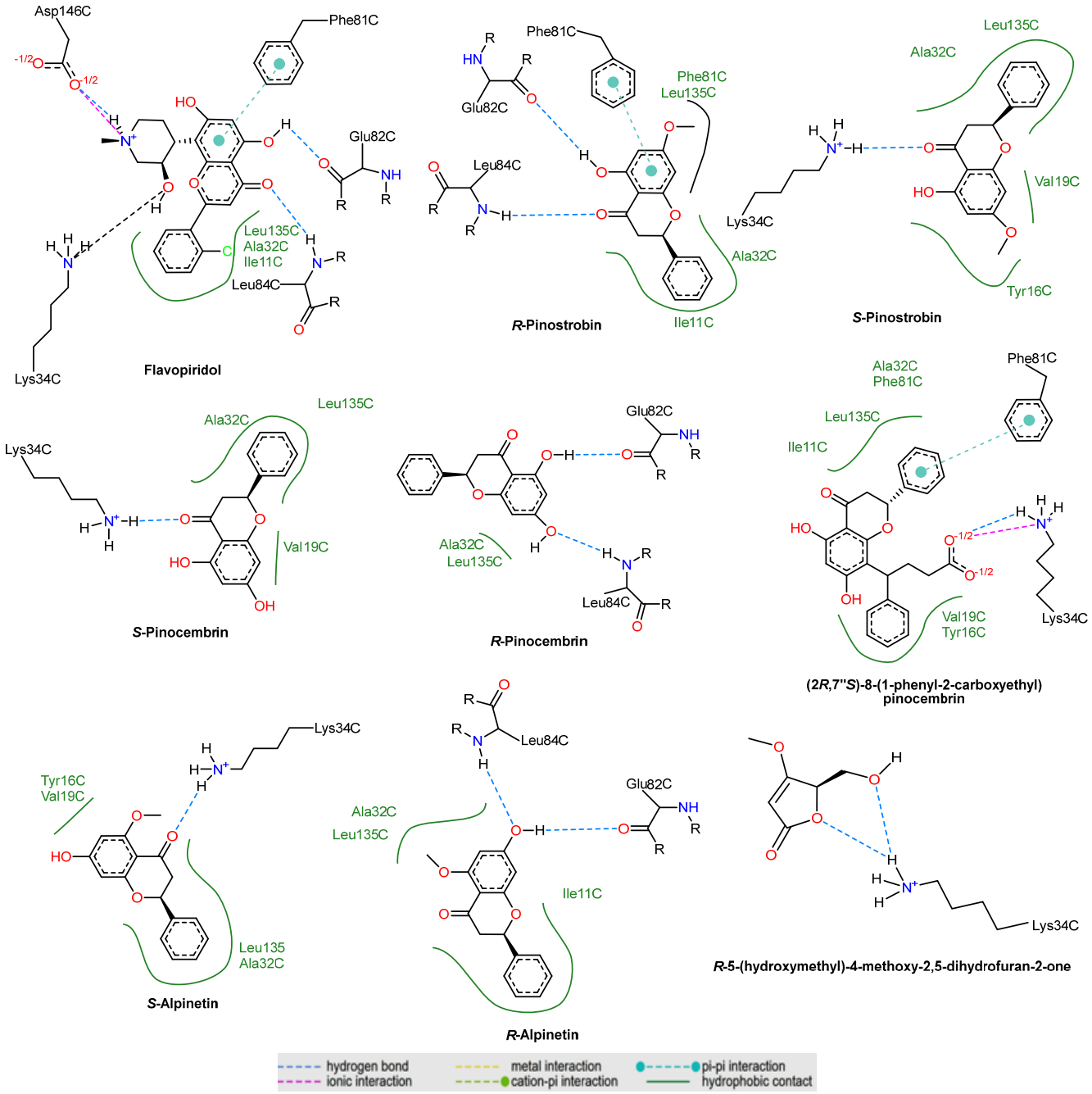


Fig 5. Two-dimensional ligand-receptor interaction diagrams of selected flavonoid compounds from *B. rotunda* with (pinostrobin, pinocembrin, alpinetin, compounds) CDK2/cyclin A complex. The interactions highlight key hydrogen bonds, hydrophobic contacts, and π–π stacking within the ATP-binding pocket, illustrating the binding orientation and molecular interaction profiles of each flavonoid

the physicochemical properties of these bioactive compounds, such as solubility and stability, which are common limitations of natural products. Therefore, the docking results represent the intrinsic binding potential of flavonoids rather than nanoparticle-bound systems. The potential enhancement of biological efficacy through AuNP-based delivery remains a separate consideration and was not directly evaluated in this study.

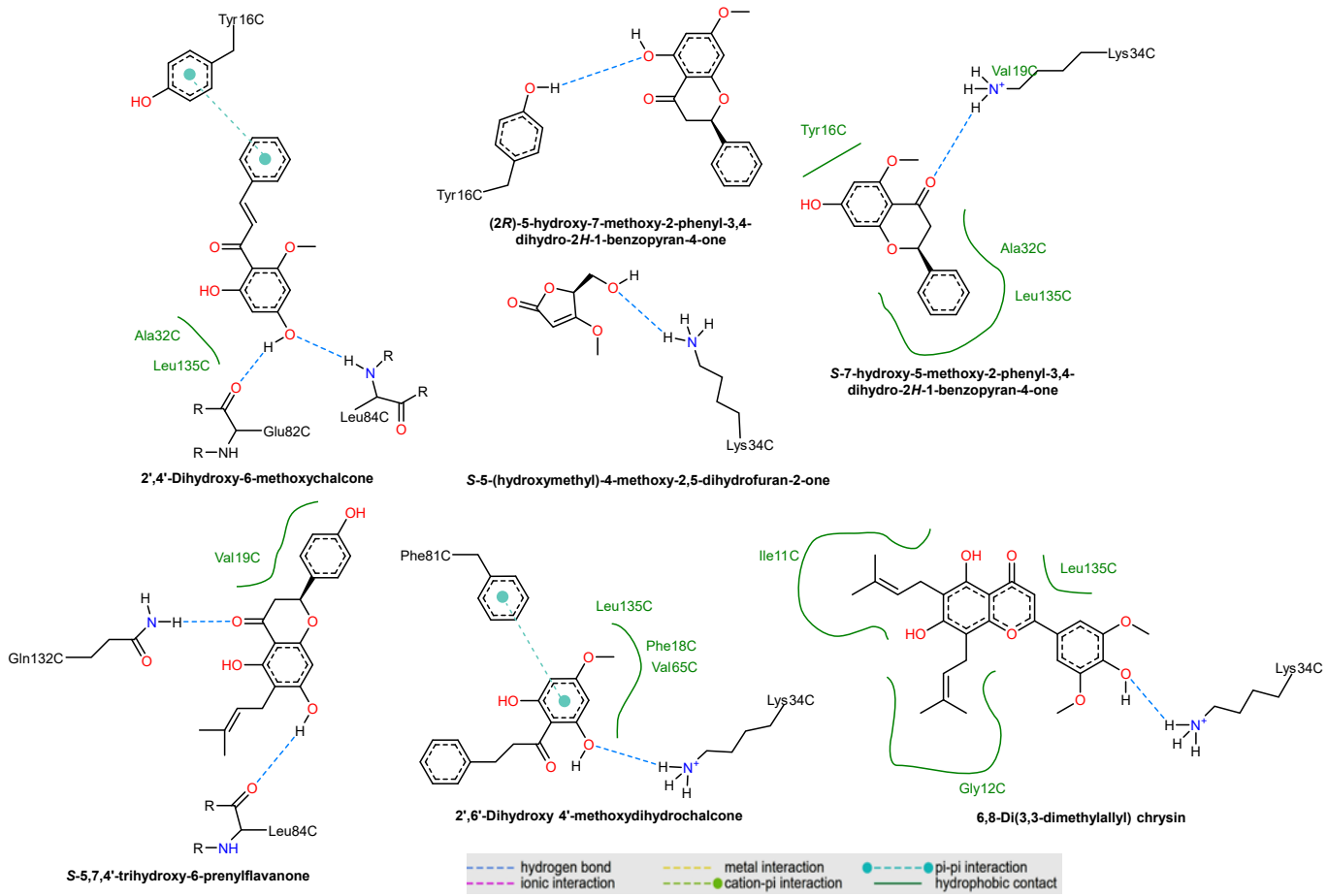


Fig 6. Two-dimensional ligand-receptor interaction diagrams of selected flavonoid compounds from *B. rotunda* (chalcone, flavanone, chrysin compounds) with CDK2/cyclin A complex. The interactions highlight key hydrogen bonds, hydrophobic contacts, and π–π stacking within the ATP-binding pocket, illustrating the binding orientation and molecular interaction profiles of each flavonoid

Antioxidant Activity

The antioxidant potential of the *B. rotunda* extracts and its Br-AuNPs was determined using the ABTS radical scavenging assay, as shown in Fig. 7. Both samples exhibited a concentration-dependent increase in scavenging activity, demonstrating that higher concentrations led to stronger ABTS radical inhibition. Across all tested concentrations, Br-AuNPs consistently exhibited superior antioxidant activity compared to the crude extract, demonstrating that conjugation with AuNPs markedly enhances the radical scavenging efficacy of *B. rotunda* bioactive compounds.

At the highest tested concentration (120 µg/mL), Br-AuNPs achieved approximately 69.4% ABTS radical scavenging activity, while the crude extract recorded around 56.2%. This pattern persisted at lower concentrations, with Br-AuNPs maintaining significantly higher activity ($p < 0.05$) even at 0.9375 µg/mL, where it showed 30.84% inhibition compared to 8.0% for the extract. The IC_{50} values were estimated from the dose–response curves, yielding approximately 10.31 µg/mL for Br-AuNPs and 86.79 µg/mL for the crude extract. Ascorbic acid was used as a standard reference antioxidant in the same ABTS assay, exhibiting a significantly lower IC_{50} value (1.29 µg/mL) compared to Br-AuNPs and the crude extract. This result confirms that although Br-AuNPs show enhanced antioxidant activity relative to the extract, their activity remains lower than that of a pure standard antioxidant. The significantly lower IC_{50} value of

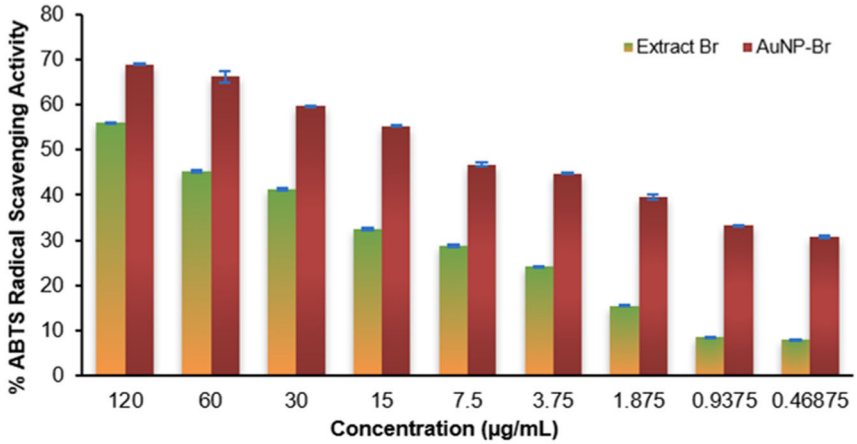


Fig 7. ABTS radical scavenging activity of methanolic extract *B. rotunda* (extract Br) and its gold nanoparticle conjugate (Br-AuNPs). Data are presented as mean ± SD (n = 3). Br-AuNPs exhibited significantly higher antioxidant activity than crude extract across all tested concentrations ($p < 0.05$)

Br-AuNPs indicates a markedly enhanced antioxidant activity compared to the extract, confirming the beneficial effect of nanoparticle formation on radical scavenging efficiency. The observed enhancement in antioxidant capacity is attributable to the synergistic interaction between *B. rotunda* phytoconstituents including flavonoids onto the AuNPs surface. The nanoscale dimensions and high surface-to-volume ratio of AuNPs enable more efficient electron transfer and stronger binding interactions of antioxidant molecules and ABTS radicals.

The antioxidant mechanism is primarily based on the ability of phytoconstituents, particularly flavonoids such as pinostrobin, chrysin, panduratin A, pinocembrin, and cardamonin, to donate electrons or hydrogen atoms to neutralize $ABTS^{\bullet+}$ radicals, converting them into their non-radical form. In the Br-AuNPs system, these phytochemicals are associated with the nanoparticle surface, which provides a high surface-to-volume ratio that facilitates interaction with radical species. Additionally, the AuNP's core may promote electron transfer processes, further enhancing radical scavenging activity [9,28].

These findings are consistent with earlier reports, Rokkarukala et al. [62] observed that *Sarcophyton crassocaule*-mediated AuNPs exhibited higher antioxidant activity than the crude extract, attributed to the adsorption of bioactive molecules on the nanoparticle surface [62]. Likewise, Muniyappan et al. [28] demonstrated that curcumin–AuNP conjugates exhibited higher inhibition values than pure curcumin across all concentrations [4]. Collectively, the present results confirm that *B. rotunda* mediated AuNPs possess enhanced radical scavenging properties through synergistic effects between phytochemicals and the AuNP surface. This improvement underscores their potential application as natural antioxidant nanomaterials for functional foods and nutraceutical formulations.

In line with the findings of Rokkarukala et al. [62], AuNPs synthesized using *Sarcophyton crassocaule* extract (SCE) exhibited stronger antioxidant activity than the crude extract. The adsorption of bioactive molecules from SCE onto spherical SCE–AuNPs with a larger surface area was proposed to contribute to this enhancement. Similarly, Oueslati et al. [31] reported that biologically synthesized nanoparticles possess elevated free radical scavenging activity due to their large surface area-to-volume ratio. In another study, Muniyappan et al. [28] demonstrated that curcumin conjugated with AuNPs (CUR–AuNPs) showed consistently higher inhibition values than pure curcumin at all tested concentrations, confirming that conjugation with AuNPs can significantly improve the antioxidant capacity of natural compounds. The improved efficiency of radical scavenging may result from the accelerated

electron transfer from hydroxyl groups of active compounds to radicals, as well as stabilization of phenoxyl radicals on the AuNP surface. Furthermore, the extensive surface area of AuNPs allows a greater number of active molecules, such as pinostrobin, to interact with free radicals, while the synergistic interaction between the gold surface and phenolic compounds enhances radical neutralization efficiency.

Discussion

The green synthesis of AuNPs using *B. rotunda* not only demonstrates a sustainable approach to nanoparticle production but also offers an avenue to integrate the intrinsic bioactivity of plant-derived flavonoids into nanomaterial design. This method is considered environmentally friendly as it employs phytochemicals as natural reducing and stabilizing agents, thereby avoiding the use of hazardous chemicals commonly required in conventional synthesis methods. The successful formation of Br-AuNPs, indicated by the SPR peak around 538–542 nm, and their spherical morphology with an average diameter of 14.35 ± 3.16 nm, is consistent with previously reported phytochemical-mediated syntheses [9,11,63].

This research highlights the significant potential of *B. rotunda* extract as a bioreductant and stabilizing agent in the synthesis of Br-AuNPs. The color transformation of the solution, as well as the SPR peak at 538–542 nm showed the successful biosynthesis of AuNPs, with flavonoids facilitating both the reduction and stabilization process. Further characterization using FTIR, DLS, and TEM revealed that the synthesized AuNPs are small, uniformly distributed, and exhibit suitable morphology for biomedical applications.

This study further explored the interaction of major flavonoids from this extract with the CDK2/cyclin A complex using an *in silico* molecular docking approach. Molecular docking targeting the CDK2/cyclin A complex, a key regulator of cell cycle progression, indicated that 6,8-di-(3,3-dimethylallyl)chrysin exhibited the lowest docking score (−63.30 kcal/mol), suggesting the most favorable predicted interaction among the tested flavonoids. These interactions suggest potential binding at the ATP-binding site of CDK2, particularly through sterically favorable interactions enabled by the dimethylallyl substituents at positions C-6 and C-8. Such hydrophobic groups may enhance ligand orientation within the binding pocket and increase lipophilicity, which are important factors influencing membrane permeability and pharmacokinetic behavior of bioactive molecules [5-6,27,32]. This observation is consistent with previous reports that prenylated flavonoids often exhibit improved anticancer and enzyme inhibitory activity due to enhanced target affinity and cellular uptake [18,26-27].

The integration of green nanotechnology and computational drug discovery highlights the potential role of *B. rotunda* in anticancer-related research. Br-AuNPs enable eco-friendly synthesis while enhancing antioxidant activity, as demonstrated in this study, through the capping phytochemicals. Altogether, the *in silico* data suggest that *B. rotunda* flavonoids exhibit moderate binding potential toward CDK2/cyclin A, with compound 14 emerging as the most promising candidate. These findings provide a rational foundation for further pharmacological exploration, including experimental validation through biochemical assays and cellular models to elucidate the full anticancer mechanism. It is important to note that the molecular docking analysis was conducted on free flavonoid compounds and does not represent the behavior of flavonoids when associated with AuNPs. Therefore, the potential CDK2 inhibitory activity of Br-AuNPs remains hypothetical and requires further experimental validation. Should any of these compounds demonstrate significant *in vitro* anticancer activity, their mechanism may involve binding to alternative targets or allosteric sites of CDK2, intracellular metabolism leading to the formation of more active metabolites, or synergistic modulation of multiple molecular pathways beyond CDK2 inhibition [37,64].

These findings support the potential advantages of green biosynthesis approaches in producing environmentally friendly and biocompatible nanomaterials, with potential applications in biomedical fields, including anticancer research [46]. However, the transition from laboratory to clinical applications faces

challenges, including the need for *in vivo* studies to confirm the efficacy and safety of AuNPs, as well as optimization of nanoparticle features to enhance their biological activity. By combining experimental and *in silico* methods, this research provides a preliminary foundation for the development of nanomaterial-based strategies in anticancer research.

The experimental results confirm the successful synthesis and enhanced antioxidant activity of Br-AuNPs. In parallel, molecular docking analysis suggests that flavonoid compounds from *B. rotunda* have the potential to interact with the CDK2 active site. However, these computational findings represent preliminary predictions and do not directly confirm biological activity. In addition to the physicochemical properties, the antioxidant potential of the synthesized Br-AuNPs was evaluated using the ABTS radical scavenging assay. As shown in Fig. 5, both the *B. rotunda* extract and Br-AuNPs exhibited concentration-dependent scavenging activity, where higher concentrations corresponded to stronger ABTS radical inhibition. The ABTS assay evaluates antioxidant activity based on the ability of compounds to donate electrons and neutralize $ABTS^{\bullet+}$ radicals, resulting in a decrease in absorbance at 734 nm. This method is widely used to assess the radical scavenging capacity of AuNPs. Previous studies have reported that green-synthesized AuNPs exhibit notable antioxidant activity, with IC_{50} values of 54.39 μg/mL for *Citrus limetta*-mediated AuNPs and 44.81 μg/mL for mycosynthesized AuNPs derived from *Aspergillus terreus*.

In this study, Br-AuNPs demonstrated significantly enhanced antioxidant activity compared to the crude extract across all tested concentrations. At the highest concentration (120 μg/mL), Br-AuNPs achieved approximately 69.4% ABTS radical scavenging activity, while the crude extract showed 56.2%. This trend persisted at lower concentrations, where Br-AuNPs consistently exhibited higher activity ($p < 0.05$), including at 0.9375 μg/mL (30.84% vs. 8.0%). The IC_{50} values estimated from the dose–response curves further confirmed this enhancement, with Br-AuNPs showing a markedly lower IC_{50} (10.31 μg/mL) compared to the crude extract (86.79 μg/mL). This substantial reduction indicates a significantly improved antioxidant efficiency upon nanoparticle formation. When compared to previously reported plant-mediated AuNPs, the Br-AuNPs in this study exhibit relatively strong antioxidant performance, suggesting competitive efficacy among green-synthesized nanoparticle systems. The nanoscale size and high surface-to-volume ratio of AuNPs facilitate more efficient electron transfer and increase the availability of active sites for interaction with ABTS radicals. However, it should be noted that this enhancement reflects *in vitro* antioxidant capacity and does not necessarily represent biological activity *in vivo*.

Notably, Br-AuNPs displayed significantly higher antioxidant activity than the crude extract at all concentrations. This enhancement can be attributed to the synergistic interaction between phytochemicals, mainly flavonoids such as alpinetin, chrysin, pinostrobin, panduratin A, and cardamonin and the AuNP surface. The nanoscale size and large surface area of AuNPs facilitate efficient electron transfer and stronger radical quenching, while conjugation with the metal surface increases stability and prevents oxidative degradation of antioxidant molecules. These findings confirm that biogenic AuNPs retain and amplify the antioxidant functionality of *B. rotunda*, positioning them as promising candidates for bioactive delivery systems and functional food fortification.

Moreover, this study reinforces the concept that green-synthesized AuNPs functionalized with bioactive flavonoids may serve a dual role not only as nanocarriers, but also as cotherapeutic agents with intrinsic anticancer properties. Taken together, the docking data suggest that flavonoids from *B. rotunda* have the potential to interact with the CDK2 active site. However, since the molecular docking analysis was performed on free flavonoid compounds, the potential CDK2 inhibitory activity of Br-AuNPs remains hypothetical and requires further experimental validation [36-37,40,64]. In conclusion, the present findings offer a rational foundation for advancing selected flavonoids from *B. rotunda* into experimental validation pipelines, including *in vitro* kinase assays, cell cycle analysis, and cytotoxicity studies in cancer cell

lines. This integrated approach is expected to facilitate the development of novel anticancer therapeutics with improved selectivity, safety, and efficacy.

■ CONCLUSION

This study successfully demonstrated the green synthesis of spherical gold nanoparticles (Br-AuNPs) using ethanolic extracts of *B. rotunda*, a flavonoid-rich medicinal plant. The synthesized Br-AuNPs exhibited good physicochemical stability, uniform morphology, and enhanced antioxidant activity compared to the crude extract, as confirmed by the ABTS radical scavenging assay. Molecular docking analysis indicated that key flavonoids from *B. rotunda*, particularly 6,8-di-(3,3-dimethylallyl)chrysin, exhibited favorable predicted interactions with the CDK2/cyclin A complex, although their binding affinity remained lower than that of the reference inhibitor flavopiridol. The molecular docking results should be considered as preliminary predictions, and further experimental validation is required to confirm the proposed biological activity. Overall, these findings highlight the potential of *B. rotunda* as an eco-friendly reducing agent for nanoparticle synthesis and as a source of bioactive flavonoids with antioxidant and potential anticancer activity. The combination of green-synthesized AuNPs and plant-derived compounds provides a promising platform for future nanomaterial-based biomedical applications. Further *in vitro* and *in vivo* studies are necessary to validate their efficacy and safety.

■ ACKNOWLEDGMENTS

This research was supported by *Beasiswa Pendidikan Indonesia* (The Indonesian Education Scholarship), *Pusat Pelayanan Pembiayaan dan Asesmen Pendidkan Tinggi* (Center for Higher Education Funding and Assessment), Ministry of Higher Education, Science, and Technology of the Republic of Indonesia, and *Lembaga Pengelola Dana Pendidikan* (Endowment Fund for Education Agency), Ministry of Finance of the Republic of Indonesia under contract No. 01056/J5.2.3./BPI.06/9/2022.

■ CONFLICT OF INTEREST

The authors declare no conflicts of interest.

■ AUTHOR CONTRIBUTIONS

Mochamad Zakki Fahmi: Supervision, study conception and design, analysis and interpretation of results, draft manuscript preparation, review & editing; Afaf Baktir: study conception and design, analysis and interpretation of results, review & editing; Dini Nur Fauzia: data collection, draft manuscript preparation, analysis and interpretation of results; Titik Taufikurohmah: analysis and interpretation of results, review & editing, Intan Permata Sari: data collection, interpretation of results, & editing; Dzikra Nasyaya Mahfudhah: data collection, interpretation of results. All authors agreed to the final version of this manuscript.

■ REFERENCES

[1] Abdulateef, S.A., Raypah, M.E., Omar, A.F., Mat Jafri, M.Z., Ahmed, N.M., Mohd Kaus, N.H., Seeni, A., Mail, M.H., Tabana, Y., Ahmed, M., Al Rawashdah, S., and Barakat, K., 2023, Rapid synthesis of bovine serum albumin-conjugated gold nanoparticles using pulsed laser ablation and their anticancer activity on HeLa cells, *Arabian J. Chem.*, 16 (11), 104395.

[2] Fahmi, M.Z., Wibowo, D.L.N., Sakti, S.C.W., Lee, H.V., and Isnaeni, I., 2020, Human serum albumin capsulated hydrophobic carbon nanodots as staining agent on HeLa tumor cell, *Mater. Chem. Phys.*, 239, 122266.

[3] D'Angelo, N.A., Noronha, M.A., Kurnik, I.S., Câmara, M.C.C., Vieira, J.M., Abrunhosa, L., Martins, J.T., Alves, T.F.R., Tundisi, L.L., Ataide, J.A., Costa, J.S.R., Jozala, A.F., Nascimento, L.O., Mazzola, P.G., Chaud, M.V., Vicente, A.A., and Lopes, A.M., 2021, Curcumin encapsulation in nanostructures for cancer therapy: A 10-year overview, *Int. J. Pharm.*, 604, 120534.

[4] Sengani, M., Grumezescu, A.M., and Rajeswari, V.D., 2017, Recent trends and methodologies in gold nanoparticle synthesis – A prospective review on drug delivery aspect, *OpenNano*, 2, 37–46.

[5] Shamloo, H.B., Jafarzadeh, S., Jouyban, A., and Soleymani, J., 2022, Synthesis and application of concanavalin A-conjugated green luminescent gold

nanoparticle/fluorescent polydopamine nanoparticles for specific differentiation of cancer cells from normal cells using glycan bioreceptors, *Mater. Chem. Phys*., 288, 126344.

[6] Badi'ah, H.I., Puspaningsih, N.N.T., Supriyanto, G., and Nasronudin, N., 2023, Rapid colorimetric sensor based on gold nanoparticles functionalized 4-amino-3-hydrazino-5-mercapto-1,2,4-triazole for cortisol detection in saliva sample, *Indones. J. Chem*., 23 (4), 1009–1020.

[7] Hammami, I., Alabdallah, N.M., Al Jomaa, A., and Kamoun, M., 2021, Gold nanoparticles: Synthesis, properties and applications, *J. King Saud Univ., Sci.*, 33, 101560.

[8] Mobaraki, M., Ghaffari, M., Zarebkohan, A., Gholipourmalekabadi, M., Fallah Omrani, V., Urbanska, A.M., and Seifalian, A., 2017, Targeted drug delivery based on gold nanoparticle derivatives, *Curr. Pharm. Des*., 23 (20), 2918–2929.

[9] Patil, T.P., Vibhute, A.A., Patil, S.L., Dongale, T.D., and Tiwari, A.P., 2023, Green synthesis of gold nanoparticles via *Capsicum annum* fruit extract: Characterization, antiangiogenic, antioxidant and anti-inflammatory activities, *Appl. Surf. Sci. Adv.*, 13, 100372.

[10] Paiva-Santos, A.C., Herdade, A.M., Guerra, C., Peixoto, D., Pereira-Silva, M., Zeinali, M., Mascarenhas-Melo, F., Paranhos, A., and Veiga, F., 2021, Plant-mediated green synthesis of metal-based nanoparticles for dermopharmaceutical and cosmetic applications, *Int. J. Pharm.*, 596, 120311.

[11] Elbialy, N.S., Abdelfatah, E.A., and Khalil, W.A., 2019, Antitumor activity of curcumin-green synthesized gold nanoparticles: *In vitro* study, *BioNanoScience,* 9 (4), 813–820.

[12] Kshtriya, V., Koshti, B., and Gour, N., 2021, Green synthesized nanoparticles: Classification, synthesis, characterization, and applications, *Compr. Anal. Chem.*, 94, 173–222.

[13] Veeramani, S., Narayanan, A.P., Yuvaraj, K., Sivaramakrishnan, R., Pugazhendhi, A., Rishivarathan, I., Jose, S.P., and Ilangovan, R., 2022, *Nigella sativa* flavonoids surface coated gold NPs (Au-NPs) enhancing antioxidant and anti-diabetic activity, *Process Biochem.*, 114, 193–202.

[14] Rodríguez-Arce, E., and Saldías, M., 2021, Antioxidant properties of flavonoid metal complexes and their potential inclusion in the development of novel strategies for the treatment against neurodegenerative diseases, *Biomed. Pharmacother.*, 143, 112236.

[15] Omolaja, A.A., Pearce, B., Omoruyi, S.I., Badmus, J.A., Ismail, E., Marnewick, J., Botha, S., Benjeddou, M., Ekpo, O.E., and Hussein, A.A., 2021, The potential of chalcone-capped gold nanoparticles for the management of diabetes mellitus, *Surf. Interfaces*, 25, 101251.

[16] Sulaiman, G.M., Waheeb, H.M., Jabir, M.S., Khazaal, S.H., Dewir, Y.H., and Naidoo, Y., 2020, Hesperidin loaded on gold nanoparticles as a drug delivery system for a successful biocompatible, anti-cancer, anti-inflammatory and phagocytosis inducer model, *Sci. Rep*., 10 (1), 9362.

[17] Khan, I., Saeed, K., and Khan, I., 2019, Nanoparticles: Properties, applications and toxicities, *Arabian J. Chem.*, 12 (7), 908–931.

[18] Kopustinskiene, D.M., Jakstas, V., Savickas, A., and Bernatoniene, J., 2020, Flavonoids as anticancer agents, *Nutrients*, 12 (2), 457.

[19] Christena, L.R., Subramaniam, S., Vidhyalakshmi, M., Mahadevan, V., Sivasubramanian, A., and Nagarajan, S., 2015, Dual role of pinostrobin-a flavonoid nutraceutical as an efflux pump inhibitor and antibiofilm agent to mitigate food borne pathogens, *RSC Adv.*, 5 (76), 61881–61887.

[20] Patel, N.K., Jaiswal, G., and Bhutani, K.K., 2016, A review on biological sources, chemistry and pharmacological activities of pinostrobin, *Nat. Prod. Res.*, 30 (18), 2017–2027.

[21] Singh, S., Meena, A., Luqman, S., and Meena, A., 2021, Acacetin and pinostrobin as a promising inhibitor of cancer-associated protein kinases, *Food Chem. Toxicol.*, 151, 112091.

[22] Jaudan, A., Sharma, S., Abd Malek, S.N., and Dixit, A., 2018, Induction of apoptosis by pinostrobin in human cervical cancer cells: Possible mechanism of

action, *PLoS One*, 13 (2), e0191523.

[23] Roman Junior, W.A., Gomes, D.B., Zanchet, B., Schönell, A.P., Diel, K.A.P., Banzato, T.P., Ruiz, A.L.T.G., Carvalho, J.E., Neppel, A., Barison, A., and Santos, C.A.M., 2017, Antiproliferative effects of pinostrobin and 5,6-dehydrokavain isolated from leaves of *Alpinia zerumbet*, *Rev. Bras. Farmacogn.*, 27 (5), 592–598.

[24] Jadaun, A., Sharma, S., Verma, R., and Dixit, A., 2019, Pinostrobin inhibits proliferation and induces apoptosis in cancer stem-like cells through a reactive oxygen species-dependent mechanism, *RSC Adv.*, 9 (21), 12097–12109.

[25] Sopanaporn, J., Suksawatamnuay, S., Sardikin, A., Lengwittaya, R., Chavasiri, W., Miyakawa, T., and Yompakdee, C., 2020, Pinostrobin suppresses the Ca^{2+}-signal-dependent growth arrest in yeast by inhibiting the Swe1-mediated G_2 cell-cycle regulation, *FEMS Yeast Res*, 20 (4), foaa026.

[26] Talib, W.H., Abuawad, A., Thiab, S., Alshweiat, A., and Mahmod, A.I., 2022, Flavonoid-based nanomedicines to target tumor microenvironment, *OpenNano,* 8, 100081.

[27] Khan, A.U., Dagur, H.S., Khan, M., Malik, N., Alam, M., and Mushtaque, M., 2021, Therapeutic role of flavonoids and flavones in cancer prevention: Current trends and future perspectives, *Eur. J. Med. Chem. Rep.*, 3, 100010.

[28] Muniyappan, N., Pandeeswaran, M., and Amalraj, A., 2021, Green synthesis of gold nanoparticles using *Curcuma pseudomontana* isolated curcumin: Its characterization, antimicrobial, antioxidant and anti-inflammatory activities, *Environ. Chem. Ecotoxicol.*, 3, 117–124.

[29] Cirillo, G., Curcio, M., Vittorio, O., Iemma, F., Restuccia, D., Spizzirri, U.G., Puoci, F., and Picci, N., 2016, Polyphenol conjugates and human health: A perspective review, *Crit. Rev. Food Sci. Nutr.*, 56 (2), 326–337.

[30] Brown, S.D., Nativo, P., Smith, J.A., Stirling, D., Edwards, P.R., Venugopal, B., Flint, D.J., Plumb, J.A., Graham, D., and Wheate, N.J., 2010, Gold nanoparticles for the improved anticancer drug delivery of the active component of oxaliplatin, *J. Am. Chem. Soc.*, 132 (13), 4678–4684.

[31] Oueslati, M.H., Ben Tahar, L., and Harrath, A.H., 2020, Catalytic, antioxidant and anticancer activities of gold nanoparticles synthesized by kaempferol glucoside from *Lotus leguminosae*, *Arabian J. Chem.*, 13 (1), 3112–3122.

[32] Kumar, S., and Pandey, A.K., 2013, Chemistry and biological activities of flavonoids: An overview, *Sci. World J.*, 2013 (1), 162750.

[33] Amawi, H., Ashby, C.R., and Tiwari, A.K., 2017, Cancer chemoprevention through dietary flavonoids: What's limiting?, *Chin. J. Cancer*, 36 (1), 50.

[34] Mir, S.A., Dar, A., Hamid, L., Nisar, N., Malik, J.A., Ali, T., and Bader, G.N., 2024, Flavonoids as promising molecules in the cancer therapy: An insight, *Curr. Res. Pharmacol. Drug Discovery*, 6, 100167.

[35] Solanki, P., Sarwadia, S., Athar, M., Jha, P.C., and Manhas, A., 2024, Targeting the cyclin-dependent kinase family in anticancer drug discovery: From computational to experimental studies, *Chem. Phys. Impact*, 9, 100768.

[36] Tadesse, S., Anshabo, A.T., Portman, N., Lim, E., Tilley, W., Caldon, C.E., and Wang, S., 2020, Targeting CDK2 in cancer: Challenges and opportunities for therapy, *Drug Discovery Today*, 25 (2), 406–413.

[37] Zhang, J., Gan, Y., Li, H., Yin, J., He, X., Lin, L., Xu, S., Fang, Z., Kim, B., Gao, L., Ding, L., Zhang, E., Ma, X., Li, J., Li, L., Xu, Y., Horne, D., Xu, R., Yu, H., Gu, Y., and Huang, W., 2022, Inhibition of the CDK2 and cyclin A complex leads to autophagic degradation of CDK2 in cancer cells, *Nat. Commun.*, 13 (1), 2835.

[38] Ali Chohan, T., Qian, H., Pan, Y., and Chen, J.Z., 2015, Cyclin-dependent kinase-2 as a target for cancer therapy: Progress in the development of CDK2 inhibitors as anti-cancer agents, *Curr. Med. Chem.*, 22 (2), 237–263.

[39] Kwon, S., Bae, H., Jo, J., and Yoon, S., 2019, Comprehensive ensemble in QSAR prediction for drug discovery, *BMC Bioinf.*, 20 (1), 521.

[40] Radini, I.A.M., Ibrahim, D.A., and Khidre, R.E., 2019, Design, synthesis and biological estimation of innovative pyrazoles as anticancer agents targeting CDK2, *Acta Pol. Pharm.*, 76 (3), 453–468.

[41] Xing, F., Wang, Z., Bahadar, N., Wang, C., and Wang, X.D., 2024, Molecular insights into kaempferol derivatives as potential inhibitors for CDK2 in colon cancer: Pharmacophore modeling, docking, and dynamic analysis, *Front. Chem.*, 12, 1440196.

[42] Stringhetta, G.R., Mass, E.B., Faria Gomes, I.N., Fonseca Peixoto, M.C., Tejada, A.H., Susucchi, L., Alves Bezerra, A.J., Silva Resende, P.V., Vendrúsculo, V., Reis, R.M., Russowsky, D., and Oliveira, R.J.D.S., 2025, Design, synthesis and evaluation of quinazoline-chalcone hybrids as inducers of cell-cycle arrest and apoptosis in breast cancer via DNA damage and CDK2/ATR inhibition, *Eur. J. Med. Chem. Rep.*, 13, 100250.

[43] Rahman, S., Talukdar, N.C., Patowary, K., and Mohanta, Y.K., 2024, Propolis from the North-East region of India exhibits potent antioxidant and anticancer activity against breast cancer cells, *Biocatal. Agric. Biotechnol.*, 59, 103269.

[44] Liu, J.Z., Lyu, H.C., Fu, Y.J., Jiang, J.C., and Cui, Q., 2022, Simultaneous extraction of natural organic acid and flavonoid antioxidants from *Hibiscus manihot* L. flower by tailor-made deep eutectic solvent, *LWT-Food Sci. Technol.*, 163, 113533.

[45] Kanchanapiboon, J., Kongsa, U., Pattamadilok, D., Kamponchaidet, S., Wachisunthon, D., Poonsatha, S., and Tuntoaw, S., 2020, *Boesenbergia rotunda* extract inhibits *Candida albicans* biofilm formation by pinostrobin and pinocembrin, *J. Ethnopharmacol.*, 261, 113193.

[46] Vemuri, S.K., Banala, R.R., Mukherjee, S., Uppula, P., Subbaiah, G.P.V., Gurava Reddy, A.V., and Malarvilli, T., 2019, Novel biosynthesized gold nanoparticles as anti-cancer agents against breast cancer: Synthesis, biological evaluation, molecular modelling studies, *Mater. Sci. Eng., C*, 99, 417–429.

[47] Hanwell, M.D., Curtis, D.E., Lonie, D.C., Vandermeersch, T., Zurek, E., and Hutchison, G.R., 2012, Avogadro: An advanced semantic chemical editor, visualization, and analysis platform, *J. Cheminf.*, 4 (1), 17.

[48] Allen, W.J., Balius, T.E., Mukherjee, S., Brozell, S.R., Moustakas, D.T., Lang, P.T., Case, D.A., Kuntz, I.D., and Rizzo, R.C., 2015, DOCK 6: Impact of new features and current docking performance, *J. Comput. Chem.*, 36 (15), 1132–1156.

[49] Diedrich, K., Krause, B., Berg, O., and Rarey, M., 2023, PoseEdit: Enhanced ligand binding mode communication by interactive 2D diagrams, *J. Comput.-Aided Mol. Des.*, 37 (10), 491–503.

[50] Hidayati, M.D., Ersam, T., Shimizu, K., and Fatmawati, S., 2017, Antioxidant activity of *Syzygium polyanthum* extracts, *Indones. J. Chem.*, 17 (1), 49–53.

[51] Sindhu, K., Rajaram, A., Sreeram, K.J., and Rajaram, R., 2014, Curcumin conjugated gold nanoparticle synthesis and its biocompatibility, *RSC Adv.*, 4 (4), 1808–1818.

[52] Al Shehab, S., El Kurdi, R., and Patra, D., 2020, Curcumin mediated PEG thiol acid conjugated gold nanoparticles for the determination of melamine, *Microchem. J.*, 153, 104382.

[53] Shaabani, E., Amini, S.M., Kharrazi, S., and Tajerian, R., 2017, Curcumin coated gold nanoparticles: Synthesis, characterization, cytotoxicity, antioxidant activity and its comparison with citrate coated gold nanoparticles, *Nanomed. J.*, 4 (2), 115–125.

[54] Hosny, M., Eltaweil, A.S., Mostafa, M., El-Badry, Y.A., Hussein, E.E., Omer, A.M., and Fawzy, M., 2022, Facile synthesis of gold nanoparticles for anticancer, antioxidant applications, and photocatalytic degradation of toxic organic pollutants, *ACS Omega*, 7 (3), 3121–3133.

[55] Merugu, R., and Gothalwal, R., 2021, Microscopic techniques for characterisation of nanomaterials: A minireview, *Mater. Today: Proc.*, 46, 4753–4757.

[56] Augustine, R., Hasan, A., Primavera, R., Wilson, R.J., Thakor, A.S., and Kevadiya, B.D., 2020, Cellular uptake and retention of nanoparticles: Insights on particle properties and interaction with cellular components, *Mater. Today Commun.*, 25, 101692.

[57] Percoco, R.M., Schirinzi, S., Mandriota, G., Cortese, B., Gigli, G., Palamà, I.E., and Maiorano, G., 2025, Smart inorganic nanoparticles in nanomedicine: Strategies for synthesis and functionalization, *Int. J. Pharm.*, 634, 126192.

[58] Nizamov, S., Sazdovska, S.D., and Mirsky, V.M., 2022, A review of optical methods for ultrasensitive detection and characterization of nanoparticles in liquid media with a focus on the wide field surface plasmon microscopy, *Anal. Chim. Acta*, 1202, 339633.

[59] Mahmoudi, A., Kesharwani, P., Majeed, M., Teng, Y., and Sahebkar, A., 2022, Recent advances in nanogold as a promising nanocarrier for curcumin delivery, *Colloids Surf., B*, 215, 112481.

[60] McCarron, E., and Chambers, G., 2021, A review of suitable analytical technology for physio-chemical characterisation of nanomaterials in the customs laboratory, *Talanta Open*, 4, 100069.

[61] Muharrami, L.K., Santoso, M., and Fatmawati, S., 2024, Chemical profiles, *in silico* pharmacokinetic and toxicity prediction of bioactive compounds from *Boesenbergia rotunda*, *Case Stud. Chem. Environ. Eng.*, 10, 100992.

[62] Rokkarukala, S., Cherian, T., Ragavendran, C., Mohanraju, R., Kamaraj, C., Almoshari, Y., Albariqi, A., Sultan, M.H., Alsalhi, A., and Mohan, S., 2023, One-pot green synthesis of gold nanoparticles using *Sarcophyton crassocaule*, a marine soft coral: Assessing biological potentialities of antibacterial, antioxidant, anti-diabetic and catalytic degradation of toxic organic pollutants, *Heliyon*, 9 (3), e14668.

[63] Sanna, V., Pala, N., DessÌ, G., Manconi, P., Mariani, A., Dedola, S., Rassu, M., Crosio, C., Iaccarino, C., and Sechi, M., 2014, Single-step green synthesis and characterization of gold-conjugated polyphenol nanoparticles with antioxidant and biological activities, *Int. J. Nanomed.*, 9 (1), 4935–4951.

[64] Malumbres, M., and Barbacid, M., 2009, Cell cycle, CDKs and cancer: A changing paradigm, *Nat. Rev. Cancer*, 9 (3), 153–166.